Research Article

Environmental enrichment combined with fasudil promotes motor function recovery and axonal regeneration after stroke

https://doi.org/10.4103/1673-5374.313048

Date of submission: October 22, 2020

Date of decision: December 7, 2020

Date of acceptance: February 9, 2021

Date of web publication: April 23, 2021

Yi-Tong Zhu, Qun Zhang, Hong-Yu Xie, Ke-Wei Yu, Gao-Jing Xu, Si-Yue Li, Yi Wu*

Graphical Abstract *A comprehensive treatment plan of post-stroke medicine combined with rehabilitation training*

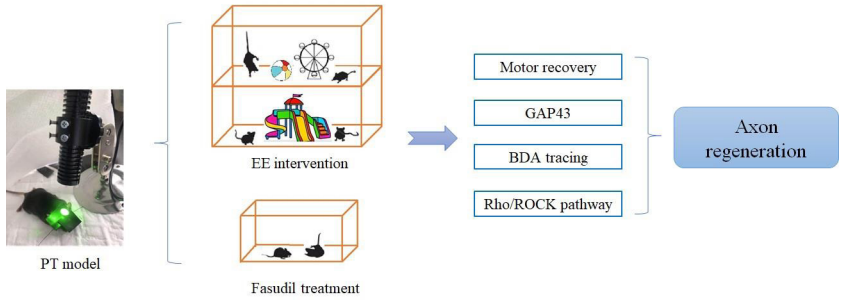

Abstract

Fasudil, a Rho-associated protein kinase (ROCK) inhibitor, has a protective effect on the central nervous system. In addition, environmental enrichment is a promising technique for inducing the recovery of motor impairments in ischemic stroke models. The present study aimed to explore whether environmental enrichment combined with fasudil can facilitate motor function recovery and induce cortical axonal regeneration after stroke. First, a mouse model of ischemic cerebral stroke was established by photochemical embolization of the left sensorimotor cortex. Fasudil solution (10 mg/kg per day) was injected intraperitoneally for 21 days after the photothrombotic stroke. An environmental enrichment intervention was performed on days 7–21 after the photothrombotic stroke. The results revealed that environmental enrichment combined with fasudil improved motor function, increased growth-associated protein 43 expression in the infarcted cerebral cortex, promoted axonal regeneration on the contralateral side, and downregulated ROCK, p-LIM domain kinase (LIMK)1, and p-cofilin expression. The combined intervention was superior to monotherapy. These findings suggest that environmental enrichment combined with fasudil treatment promotes motor recovery after stroke, at least partly by stimulating axonal regeneration. The underlying mechanism might involve ROCK/LIMK1/cofilin pathway regulation. This study was approved by the Institutional Animal Care and Use Committee of Fudan University, China (approval No. 20160858A232) on February 24, 2016.

Key Words: axon regeneration; biotinylated dextran amines; environmental enrichment; fasudil; growth-associated protein 43; ischemic stroke; motor recovery; Nissl bodies; Rho/ROCK pathway

Chinese Library Classification No. R454; R453; R741

Introduction

Stroke is a serious threat to human health and represents the second leading cause of death around the world (Campbell et al., 2019). In stroke patients, there is a limited capacity for the recovery of neurological function because of inactivated neural plasticity (Cai et al., 2020). Axonal regeneration and the re-establishment of connections is considered the basis of neural network remodeling. However, the sprouting and regeneration of axons are restricted after stroke. The main reason for this is that the regenerative ability of the central nervous system (CNS) is poor, and a harmful cellular and molecular environment forms around the injured area, which in turn affects axonal regeneration and sprouting as well as functional recovery. Reducing the production of myelin inhibitors; mitigating exogenous influencing factors such as glial scar response; and endogenously regulating Rho, phosphatase and tensin homolog, glycogen synthase kinase 3, and other signaling pathways that regulate transcription factors (such as the Krüppel-like family of transcription factors (Blackmore et al., 2012) and SRY-box transcription factor 11 (Wang et al., 2015)) may effectively promote axonal regeneration in the CNS.

An enriched environment (EE) is considered a classic and effective means of rehabilitation in rodents after stroke (Winstein et al., 2016; Wang et al., 2020). Compared with a standard environment, EE provides more sensory stimuli, increases social activities, and improves the motivation and efficiency of exercise. This artificially created complex

Department of Rehabilitation Medicine, Huashan Hospital, Fudan University, Shanghai, China

*Correspondence to: Yi Wu, PhD, wuyi@fudan.edu.cn.

https://orcid.org/0000-0003-4854-9898 (Yi Wu); https://orcid.org/0000-0003-3393-6733 (Yi-Tong Zhu)

Funding: *This study was supported by the National Natural Science Foundation of China, Nos. 81672242 (to YW), 81972141 (to YW); Shanghai Sailing Program, No. 20YF1403500 (to QZ); and Shanghai Municipal Key Clinical Specialty of China, No. shslczdzk02702 (to YW).*

How to cite this article: *Zhu YT, Zhang Q, Xie HY, Yu KW, Xu GJ, Li SY, Wu Y (2021) Environmental enrichment combined with fasudil promotes motor function recovery and axonal regeneration after stroke. Neural Regen Res 16(12):2512-2520.*

environment is more effective for stimulating the body's nerves and endocrine responses, thereby promoting the recovery of neural function (Rosbergen et al., 2019). Previous research has demonstrated that EE preconditioning improves the recovery of motor function without reducing infarct volume or edema (Xie et al., 2013). However, the mechanism by which EE promotes neural functional recovery has not yet been clearly elucidated. A preliminary experiment by our group revealed that, although the vital signs of cerebral ischemia model mice were stable in the acute period (within 24 hours after the model was created), the motor function prognosis of model mice in the intervention group was worse if EE intervention was started in this acute time period. A large, multicenter, randomized controlled clinical trial also reported that initiating rehabilitation training within 24 hours of cerebral ischemia does not have a positive effect on functional recovery, but instead induces ischemic focus progression and promotes mortality (AVERT Trial Collaboration group, 2015). For safety reasons, we therefore adjusted the EE intervention start point to 7 days after stroke induction in the present study.

Upon cerebral infarction, spontaneous reorganization and repair of the cortex around the injured area occurs. This plasticity is inseparable from the regeneration of axons. After axonal regeneration, the extension process requires the cooperation of the actin backbone and the microtubule system. The Rho/Rho-associated protein kinase (ROCK) signaling pathway participates in the assembly, movement, and maintenance of microtubules in the cytoskeleton. Within a few hours after stroke, both Rho and ROCK levels are increased in the neurons and astrocytes of the ipsilesional hemisphere of animals and humans, resulting in enhanced ROCK activity (Brabeck et al., 2003; Yano et al., 2008). Rho/ROCK activation is the most important factor for inhibiting axonal regeneration. Studies have reported that inhibiting ROCK relieves axonal regeneration inhibition caused by myelin, and promotes axonal regeneration and motor function recovery (Schmandke et al., 2007; Liu et al., 2016). Fasudil, which is considered a ROCK inhibitor, expands blood vessels in the ischemic hemisphere of the brain, protects nerve cells, and promotes axonal regeneration; it has promising treatment effects in experimental acute ischemic stroke (Lingor et al., 2007).

We hypothesized that combining early-phase (from post-photothrombotic stroke [PT] day 1) fasudil and late-phase (from post-PT day 7) EE may stimulate axonal regeneration via the ROCK pathway in a mouse model of stroke. This study explored the effects of this joint intervention on motor function in hemiplegia and on the sprouting of new axons in a photochemical embolization mouse model. We also observed whether the combination therapy was superior to a single-therapy approach, and explored its underlying mechanisms.

Materials and Methods

Animals

All animal experimental procedures were approved by the Institutional Animal Care and Use Committee of Fudan University (Shanghai, China; approval No. 20160858A232) on February 24, 2016, and followed the National Institutes of Health Guide for the Care and Use of Laboratory Animals. The experimental operator made every possible effort to minimize animal suffering.

A total of 75 clean male C57BL/6J mice, aged 8 weeks and weighing 23–25 g, were purchased from Wei Tong Li Hua Lab Animal Ltd., Beijing, China (license No. SCXK (Jing) 2019-0001). Animals had access to food and water ad libitum and were housed in the specific-pathogen-free animal experiment room at a temperature of 24 ± 2°C, with humidity of 40–70% and a 12-hour light/dark cycle. Before the PT surgery, mice were anesthetized by an intraperitoneal injection of 1% pentobarbital sodium. During surgery and the postoperative wake-up period, animals were kept warm with a heating pad set at 37°C.

Mice that met the training standards (with hemiplegic symptoms evident in the right forelimb) were allocated randomly to the following five groups (n = 15/group) using a digit table: (1) sham group: mice received the same operation as for PT but without laser irradiation, and an equal volume of saline as for the fasudil treatment (5 mL/kg); (2) PT group: mice received photochemical embolization and an equal volume of saline as for the fasudil treatment (5 mL/kg); (3) PT + EE group: mice received photochemical embolization, EE intervention, and an equal volume of saline as for the fasudil treatment (5 mL/kg); (4) PT + fasudil group: mice received photochemical embolization and fasudil treatment at 10 mg/kg per day for 3 weeks; and (5) PT + EE + fasudil group: mice received photochemical embolization, EE intervention, and fasudil treatment at 10 mg/kg per day for 3 weeks (**Figure 1**).

PT model

The PT model was induced in the left sensorimotor cortex (Zhang et al., 2019). With the mouse skull firmly fixed on the operating table in a stereotaxic locator (RWD Life Sciences, Shenzhen, China), the left sensorimotor cortex area (coordinates: rostral to caudal: 2.5 to 1.5 mm, medial to lateral: 0 to 4 mm, relative to bregma) was completely exposed, and the rest of the brain was covered with a shading plate. Immediately after injecting 0.1% rose bengal (0.01 mL/g, dissolved in 0.9% normal saline; Sigma, St. Louis, MO, USA) into the posterior bulbous vein plexus, the target area was illuminated with a green laser beam (Yunxiang Photoelectron, Zhongshan, China) at a wavelength of 532 nm for 10 minutes, at a maximum output of 50 mW. Mice in the sham group were not irradiated with the laser after the injection of rose bengal.

EE and fasudil treatments

The PT + EE and PT + EE + fasudil groups were housed in a two-story cage (30 cm × 40 cm × 40 cm) with ladder access between the floors. The cage contained a log cabin, running wheels, climbing ladders, winding tunnels, and other small toys (**Figure 1**). The types and placement of the toy objects inside the cage were updated every 3 days to maintain the novelty. Mice in the sham, PT, and PT + fasudil groups lived in groups of five animals in conventional cages (21 cm × 27 cm × 16 cm) without any decoration inside. The EE intervention started on post-PT day 7 and ended on day 21. Fasudil (2 mg/mL, MedChemExpress, Monmouth Junction, NJ, USA) was injected intraperitoneally every morning (10 mg/kg per day (Liu et al., 2016)) from post-PT days 1 to 21.

Anterograde neurotracing

On post-PT day 21, the mice in each group underwent unilateral craniotomy over the right frontal lobe and motor cortex. Biotinylated dextran amine (BDA) powder was dissolved in physiological saline to prepare a 10% BDA solution (BDA-10,000 Neuronal Tracer Kit, N7167; Thermo Fisher Scientific, Waltham, MA, USA), which was then injected into four sites of the somatosensory motor cortex of the contralesional hemisphere through finely drawn glass capillaries (600 nL/site; 0 and 0.5 mm rostral to the bregma, 1.5 and 2.0 mm lateral to the midline, 0.7 mm deep from the cortical surface (Paxinos and Franklin, 2013; Liu et al., 2014)). The needle remained in place for 10 minutes after injection. The mice were decapitated and processed for sectioning and staining after 14 days.

Behavioral assessments

Accelerating rotarod test

The rotarod test was used to test the balance, coordination,

physical conditions, and motor-planning abilities of mice (de Oliveira et al., 2020). Each mouse was trained for 3 consecutive days before surgery to ensure that all mice were able to stay on the rotarod apparatus (Yiyan Science and Technology Development Co. Ltd., Jinan, China) for 5 minutes at a speed of 40 r/min. The training method was as follows. Starting at 09:00 every day, training was performed at 5, 10, and 20 r/min for 3 minutes, at 3-minute intervals. Next, training was carried out at 40 r/min for 5 minutes at 3-minute intervals. The rotarod test was conducted on post-PT days 7, 14, and 21. No test exceeded 5 minutes, and mice were given a 3-minute rest between tests to avoid the effects of fatigue on test results. For each test, the latency to fall off the rotating rod was recorded in each group of mice, and the average of three consecutive tests was considered the final result. The experiment ended if a mouse held onto the rotating rod for three consecutive turns.

Cylinder test

The cylinder test was performed to measure spontaneous forelimb use and symmetry between the non-impaired and impaired forelimbs (Mu et al., 2019). Animals were placed in a transparent drum with a diameter of 9 cm and a height of 15 cm. When a mouse stood on its hindlimbs, the number of simultaneous initial contacts of the left forelimb, right forelimb, and both forelimbs with the cylinder wall was recorded. If one forelimb (e.g., the right forelimb) touched the cylinder wall, and then the other forelimb (the left forelimb) touched the wall before the right forelimb was removed, one right and one simultaneous touch were recorded. When both forelimbs alternately touched the wall of the cylinder, a simultaneous touch was recorded. The test was performed for 5 minutes each on post-PT days 7, 14, and 21. The laterality index (%) was calculated according to the following formula: (left + 0.5 × both)/(right + left + both) × 100. Left, right and both indicate the number of contacts of the left, right and both forelimbs.

Rung walking test

The rung walking test was used to qualitatively and quantitatively describe the limb behavior of mice, including limb placement, gait, and coordination (Zhang et al., 2019). The main body of the testing apparatus was composed of two transparent acrylic walls (69.5 cm × 15 cm) with a distance of 5 cm between them that allowed mice to pass, but was not wide enough for the mice to be able to turn around. Thirty-one metal strips with a diameter of 0.1 cm were inserted into holes in the wall, side by side, at a distance of 1 cm. Before PT, the mice were trained three times to adapt to crossing the device. The tests were conducted on post-PT days 7, 14, and 21. Both the number of slipped steps and the total number of steps of the right forelimb were recorded using SMART 3.0 software (RWD Life Sciences). The forelimb slip rate was evaluated as the ratio of the number of slipped steps to the total number of steps.

Western blot assay

On post-PT day 22, the mice were sacrificed and approximately 20 mg of tissue around the infarct was removed. Protein quantification was assessed using a bicinchoninic acid protein assay kit (G2026, Servicebio, Wuhan, China). Samples (20 μg/well) were separated using 12% sodium dodecyl sulfate-polyacrylamide gel electrophoresis and transferred to polyvinylidene difluoride membranes (Millipore, Billerica, MA, USA) using a Trans-Blot Turbo Transfer System (Bio-Rad, Berkeley, CA, USA). The membranes were then incubated in blocking buffer (5% skim milk powder in phosphate-buffered saline with 0.1% Tween-20) for 1 hour. Membranes were then incubated overnight at 4°C with rabbit anti-p-cofilin (phosphor S3; Cat# ab12866, 1:500, Abcam, Cambridge, MA, USA), anti-cofilin (Cat# ab42824, 1:2000, Abcam), anti-p-LIM domain kinase (LIMK)1 (phosphor T508; Cat# ab38508, 1:1000, Abcam), anti-LIMK1 (Cat# PA5-79603, 1:1000, Thermo Fisher Scientific), anti-ROCK (Cat# ab125025, 1:10,000, Abcam), and mouse anti-glyceraldehyde-phosphate dehydrogenase (GAPDH; Cat# ab8245, 1:6000, Abcam). After three 5-minute washes with phosphate-buffered saline containing 0.1% Tween-20, the membranes were incubated for 60 minutes at room temperature with goat anti-rabbit IgG (Cat# A0208, 1:500, BioTNT, Shanghai, China) or goat anti-mouse antibody (Cat# A0216, 1:500, BioTNT). ImageJ software (National Institutes of Health, Bethesda, MD, USA) was then used to analyze the integrated optical density values of the bands after they were developed using Odyssey (Li-COR Biosciences, Lincoln, NE, USA).

Nissl staining

Brain sections were deparaffinized using xylene, and were then placed in 100% ethanol for approximately 5 minutes, 95% ethanol for approximately 30 seconds, and 70% ethanol for approximately 30 seconds. After three washes with ultrapure water, the sections were incubated for 20 minutes in 1% toluidine blue solution (preheated to 50°C in advance) at 56°C in an incubator. After a further three washes with ultrapure water, the sections were differentiated in 70% ethanol for 1 minute, followed by 95% ethanol for a few seconds (staining was controlled under a microscope, by observing Nissl body display clarity). The Nissl-stained sections were then dehydrated, cleared, and sealed before being examined under a light microscope (Olympus, Tokyo, Japan). The Nissl-positive cell numbers were measured using ImageJ software. Surviving cells showed well-stained Nissl bodies. Damaged cells were swollen and had lost Nissl-stained material, and sometimes also had dense dendritic fragments caused by necrosis.

Immunohistochemistry

On post-PT day 22, mice (n = 3/group) were placed under deep anesthesia and their brain tissue was fixed by transcardial perfusion with 4% paraformaldehyde, followed by immersion in 4% paraformaldehyde. The brain tissue was then processed into 6 μm paraffin sections. Sections were dewaxed and rehydrated, and antigen retrieval was then performed by placing the sections into antigen repair solution (pH 9.0, ethylenediaminetetraacetic acid; Cat# 10009717, Sinopharm Chemical Reagent Co., Ltd., Shanghai, China) and heating three times for 90 seconds on high heat in a microwave oven. Sections were washed with distilled water before being incubated in 3% H_2O_2 solution for 20 minutes at room temperature to inactive endogenous peroxidases. After blocking with 10% goat serum for 30 minutes, the sections were incubated at 4°C overnight in rabbit anti-growth-associated protein 43 antibody (GAP43; Cat# NB300-143SS, 1:1000, Novus Biologicals, Centennial, CO, USA). Sections were then incubated in horseradish peroxidase-labeled goat anti-rabbit IgG (1:50; Beyotime, Shanghai, China) at 37°C for 30 minutes. Signal was developed using 3,3′-diaminobenzidine tetrahydrochloride (DAB; Cat# P0202, Beyotime). After being counterstained, dehydrated, cleared, and sealed, the sections were observed under a microscope (Olympus) and the positive areas were measured using ImageJ software.

Brain tissue used for BDA immunohistochemistry was removed 35 days after PT. The only difference in this staining method was that, after blocking, the sections were incubated in 1 g/mL avidin-horseradish peroxidase working solution (Cat# N7167, Thermo Fisher Scientific) overnight. After washing with phosphate-buffered saline, 5% DAB (Cat# N7167, Thermo Fisher Scientific) was used for signal development.

Statistical analysis

All data are expressed as the mean ± standard error of the mean (SEM). Data from the behavioral tests among the different timepoints in the five groups were analyzed using

two-way analysis of variance (ANOVA) with Tukey's *post-hoc* tests. Data from the molecular biology tests, including western blot, Nissl staining, and immunohistochemistry, were analyzed using one-way ANOVA followed by Tukey's multiple comparisons. Correlations between motor function outcomes and the p-cofilin/cofilin ratio or p-LIMK1/LIMK1 ratio were analyzed using Pearson's correlation coefficient. All statistical analyses were performed using GraphPad Prism version 6.0 (GraphPad Software Inc., San Diego, CA, USA). $P < 0.05$ was considered statistically significant.

Results

EE combined with fasudil promotes long-term motor recovery after PT

Accelerating rotarod test

Before PT surgery, all animals were trained for 3 days to run for 5 minutes on the rotating rod. Significant effects of time ($F_{(5,350)} = 272.7$, $P < 0.0001$), treatment ($F_{(4,70)} = 80.72$, $P < 0.0001$), and time × treatment interaction ($F_{(20,350)} = 28.82$, $P < 0.0001$) were observed by two-way repeated measures ANOVA (**Figure 2A**). Tukey's multiple comparisons revealed that there were no significant differences in motor ability between the groups over the 3 pre-trial training days ($P = 0.2651$). On post-PT day 7, the motor ability of mice in the PT group was significantly lower than that of the sham group, with an approximate 65% reduction in the length of time spent on the rotating rod; in addition, a protective effect of fasudil began to appear. A better performance was observed in the PT + EE group compared with the PT group on post-PT days 14 ($P < 0.0001$) and 21 ($P < 0.0001$) (**Figure 2B** and **C**). At 21 days after PT, motor ability in the PT + EE + fasudil group was similar to that of the sham group ($P = 0.8769$), but significantly higher than that of the PT + EE ($P = 0.0144$) and PT + fasudil ($P = 0.0321$) groups. Although the PT + EE and PT + fasudil groups had significantly improved exercise capacities compared with the PT group (both $P < 0.0001$), there was still a clear difference compared with the results of the sham group.

Cylinder test

Two-way repeated measures ANOVA followed by Tukey's multiple comparisons revealed the significant effects of time ($F_{(3,210)} = 29.8$, $P < 0.0001$), treatment ($F_{(4,70)} = 18.89$, $P < 0.0001$), and time × treatment interaction ($F_{(12,210)} = 2.711$, $P = 0.002$) (**Figure 2D**). On post-PT day 7, the degree of dependence on the left forelimb was significantly increased in all groups except for the sham group, and a lack of right forelimb use was apparent. On post-PT days 14 and 21, the PT + EE and PT + fasudil groups still tended to have left-forelimb dominance in terms of wall contacts, with no significant difference compared with the PT group ($P > 0.9999$ and $P = 0.1729$, respectively, on post-PT day 14; $P = 0.9993$ and $P = 0.1774$, respectively, on post-PT day 21; **Figure 2E** and **F**). In contrast, the PT + EE + fasudil group tended to use the bilateral forelimbs to simultaneously contact the wall, and the laterality index was significantly lower than that of the PT group ($P = 0.0096$ on post-PT day 14, $P = 0.0007$ on post-PT day 21), reflecting the advantages of combined intervention.

Rung walking test

A two-way ANOVA indicated significant effects of time ($F_{(3,210)} = 93.94$, $P < 0.0001$), treatment ($F_{(4, 70)} = 185$, $P < 0.0001$), and time × treatment interaction ($F_{(12, 210)} = 33.98$, $P < 0.0001$) on forelimb placement among the five groups (**Figure 2G**). On post-PT day 7, all four groups of model mice had a significant increase in the forelimb slip rate compared with the sham group (all $P < 0.0001$). On post-PT days 14 and 21, both the EE and fasudil treatment groups had a robust recovery, with no significant differences compared with the sham group at post-PT day 21 ($P = 0.2412$ and $P = 0.0752$, respectively, **Figure 2H** and **I**). Notably, the recovery of mice in the PT + EE + fasudil group was faster than that of mice in the PT + EE ($P < 0.0001$ on day 14 and $P = 0.0044$ on day 21) or PT + fasudil ($P = 0.0086$ on day 14 and $P = 0.0006$ on day 21) groups. Results from the PT + EE + fasudil group were similar to those of the sham group on post-PT days 14 and 21 (both $P > 0.05$).

EE combined with fasudil relieves neuron damage after PT

Nissl staining demonstrated that the morphology of sensorimotor cortical neurons in the sham group was normal, with Nissl bodies presenting as blue/violet plaques or granules that were evenly distributed in the cytoplasm. Compared with the sham group, the PT group had a loose peripheral area around the infarct, and significantly less neurons with a disordered arrangement. The PT + EE and PT + fasudil groups had more neurons, and more clustered neurons, compared with the PT group. Neurons in the PT + EE + fasudil group were not only significantly increased, but were also arranged in a more orderly fashion compared with those of the other three model groups. (**Figure 3**).

EE combined with fasudil promotes axonal regeneration after PT

Axonal sprouting was investigated by evaluating GAP43 immunopositivity in the ipsilesional cortex. Immunohistochemical staining at post-PT day 22 is shown in **Figure 4**. The PT + EE + fasudil group had significantly higher GAP43 immunopositivity compared with the PT group ($P = 0.0006$), indicating that the combined intervention of EE and fasudil was able to effectively stimulate axonal regeneration.

As a neuronal tracer, BDA can track neurons and their axons. Immunohistochemical staining revealed the neurons and new axons that had taken up BDA as brown/yellow signals. In each group of mice, labeled neurons and their axons were observed in the cortex, whereas the cortex around the infarct area had axon fibers only (and no labeled neurons), indicating that axon fibers originating from the contralateral cortex grew toward the ischemic cortex to compensate for its lack of function. The numbers of labeled neurons and sprouting axons in the contralateral cortex were different between the groups, with the PT + fasudil and PT + EE + fasudil groups showing higher amounts than the PT group. Compared with the PT group, the labeled axon fibers in the ipsilesional cortex of the EE group were arranged in a more orderly manner, and the number of labeled axon fibers in the PT + fasudil group was significantly higher. Notably, the labeled axon fibers in the PT + EE + fasudil group were not only the most numerous of all groups, but they were also arranged in the most orderly fashion (**Figure 5**).

EE and fasudil promote motor recovery by regulating the ROCK/LIMK1/cofilin pathway in the infarct brain after PT

One-way ANOVA revealed significant changes in ROCK levels [$F_{(4,40)} = 5.984$, $P = 0.0007$] in the cortex following EE and fasudil treatment. *Post-hoc* Tukey's multiple comparisons indicated that ROCK expression was significantly higher in the PT group compared with the sham group ($P < 0.05$); this was reversed by repeated treatment with the ROCK inhibitor fasudil for 21 days ($P < 0.05$ PT + fasudil *vs*. PT; $P < 0.001$ PT + EE + fasudil *vs*. PT; **Figure 6A**).

Mice with PT who had impaired motor ability in the tests, with or without EE and fasudil, had cortical alterations of p-LIMK1 [$F_{(4,40)} = 10.66$, $P < 0.001$], p-LIMK1/LIMK1 ratio [$F_{(4,40)} = 3.313$, $P = 0.0195$], p-cofilin [$F_{(4,40)} = 2.77$, $P = 0.0401$], and p-cofilin/cofilin ratio [$F_{(4,40)} = 5.841$, $P = 0.0008$], in a trend similar to that observed in the animal behavior experiments. LIMK1 and cofilin are potent enhancers of axonal plasticity, and their activities are lost after phosphorylation (Bernstein and Bamburg, 2010; Morin et al., 2011). A *post-hoc* Tukey's

test indicated that p-LIMK1 levels were increased in the cortex of mice in the PT group compared with the sham group ($P < 0.0001$); this trend was reversed by both fasudil ($P < 0.05$) and EE + fasudil ($P < 0.0001$). Inactivation of LIMK1 is reflected by the p-LIMK1/LIMK1 ratio, which was markedly lower in the PT + EE + fasudil group compared with the PT group (**Figure 6B**). Similarly, the p-cofilin/cofilin ratio is an index of cofilin inactivation, and was significantly lower in the PT + EE + fasudil group compared with the PT group ($P < 0.01$). Additionally, EE or fasudil treatment alone significantly reduced cofilin inactivation ($P < 0.01$ and $P < 0.05$, respectively) (**Figure 6C**).

Correlations between motor function outcomes and the p-cofilin/cofilin or p-LIMK1/LIMK1 ratios in the ipsilesional cortex

Possible correlations between motor function recovery and the levels of p-cofilin/cofilin and p-LIMK1/LIMK1 ratios in the ipsilesional cortex were assessed by comparing the latency to fall in the rotarod test and the forelimb slip rate in the rung walking test with the relative p-cofilin/cofilin and p-LIMK1/LIMK1 ratios, using Pearson's correlation coefficient. As shown in **Figure 7**, the latency to fall and the forelimb slip rate were negatively and positively correlated with the ratios of p-cofilin/cofilin and p-LIMK1/LIMK1, respectively. The correlation was stronger for p-cofilin/cofilin than for p-LIMK1/LIMK1.

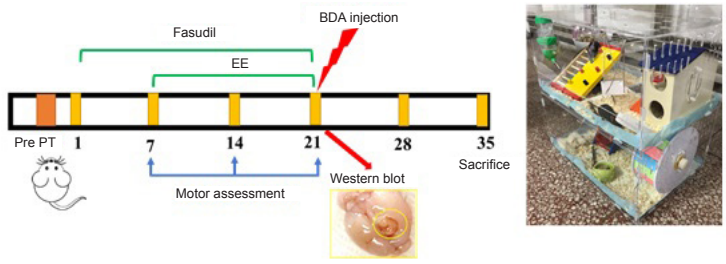

Figure 1 | **Time course of interventions (left) and the EE cage (right).**
BDA: Biotinylated dextran amines; EE: enriched environment; PT: photothrombotic stroke.

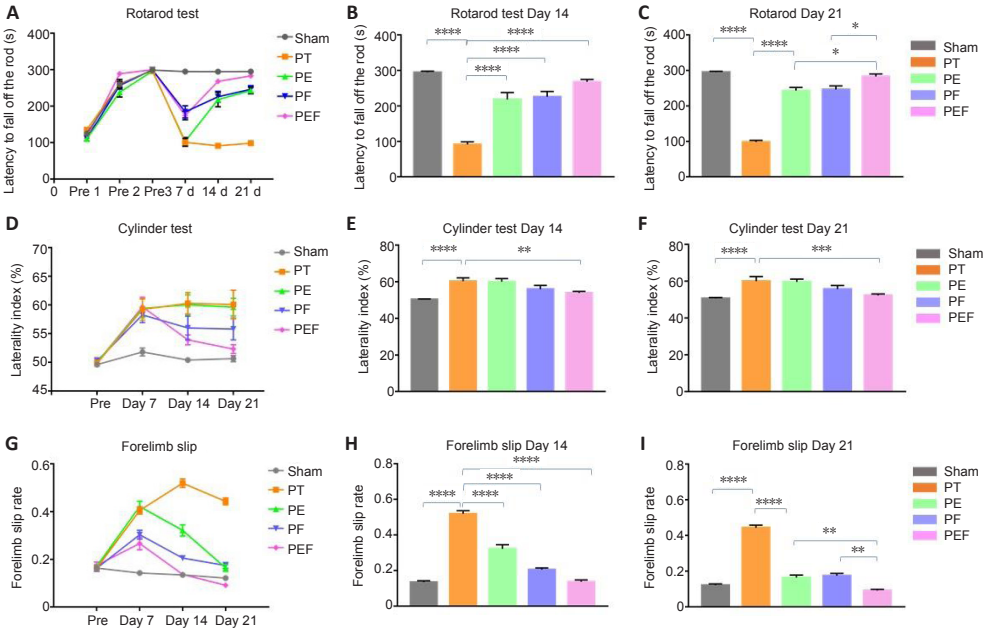

Figure 2 | **EE combined with fasudil promotes motor recovery after PT.**
(A) Latency to fall off the rod in the accelerating rotarod test. (B, C) Histogram of the latency to fall off the rod on post-PT days 14 and 21 in the accelerating rotarod test. (D) Laterality index in the cylinder test. (E, F) Histogram of the laterality index in each group on post-PT days 14 and 21 in the cylinder test. (G) Forelimb slip rate in the rung walking test. (H, I) Histogram of the forelimb slip rate in each group on post-PT days 14 and 21 in the rung walking test. EE combined with fasudil promoted the performance of model mice in the rotarod, cylinder, and forelimb slip tests. Data are expressed as the mean ± SEM ($n = 15$). *$P < 0.05$, **$P < 0.01$, ***$P < 0.001$, ****$P < 0.0001$ (two-way analysis of variance followed by Tukey's *post-hoc* test). EE: Enriched environment; PT: photothrombotic stroke. Sham group: mice received saline; PT group: mice received photochemical embolization and saline; PT + EE group (PE): mice received photochemical embolization, EE intervention, and saline; PT + fasudil group (PF): mice received photochemical embolization and fasudil treatment at 10 mg/kg per day for 3 weeks; and PT + EE + fasudil group (PEF): mice received photochemical embolization, EE intervention, and fasudil treatment at 10 mg/kg per day for 3 weeks.

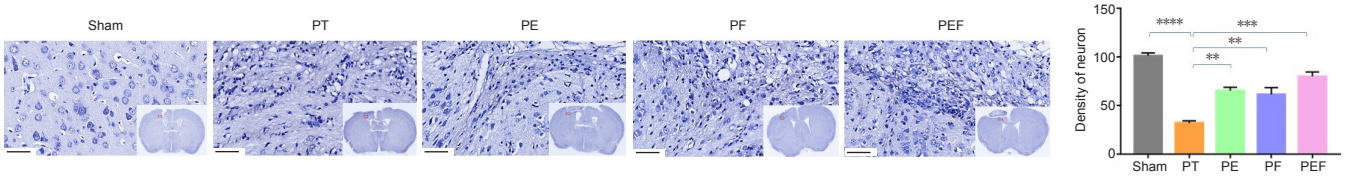

Figure 3 | **EE combined with fasudil relieves the damage in cortical neurons following PT (Nissl staining).**
Representative micrographs of Nissl staining and quantification of Nissl-stained neurons. Surviving cells showing well-stained Nissl bodies are marked with red arrows, while damaged cells forming dense necrotic dendritic fragments are marked with black arrows. The neurons in the sham group were arranged regularly, and there were almost no swollen or necrotic cells. The Nissl bodies in the cell bodies and dendrites were large and numerous, and were dyed dark blue or purple. In the PT group, the arrangement of neurons was disordered, and there were many necrotic cells. There were many darkly stained cell fragments in the cell body and dendrites, and Nissl bodies were almost invisible. The numbers of surviving neurons in the PT + EE, PT + fasudil, and PT + EE + fasudil groups were significantly higher than those in the PT group. Scale bars: 50 μm, original magnification 40×. Data are expressed as the mean ± SEM ($n = 3$). **$P < 0.01$, ***$P < 0.001$, ****$P < 0.0001$ (one-way analysis of variance followed by Tukey's multiple comparisons). EE: Enriched environment; PT: photothrombotic stroke. Sham group: mice received saline; PT group: mice received photochemical embolization and saline; PT + EE group (PE): mice received photochemical embolization, EE intervention, and saline; PT + fasudil group (PF): mice received photochemical embolization and fasudil treatment at 10 mg/kg per day for 3 weeks; and PT + EE + fasudil group (PEF): mice received photochemical embolization, EE intervention, and fasudil treatment at 10 mg/kg per day for 3 weeks.

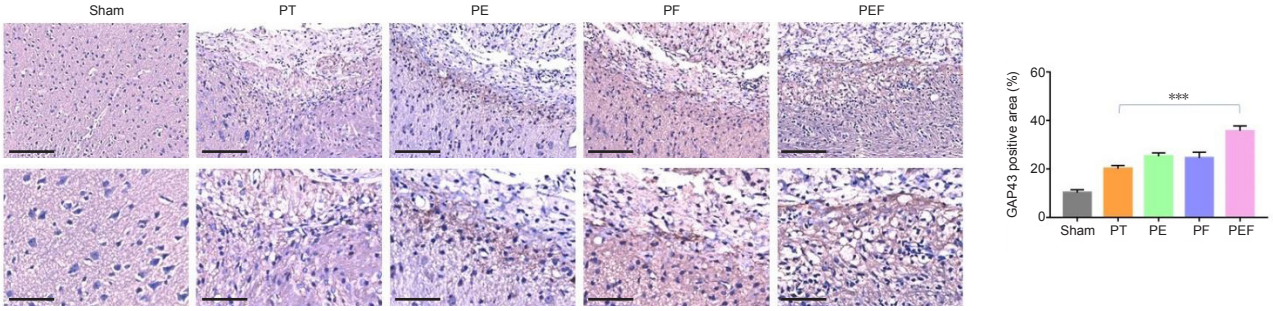

Figure 4 | EE combined with fasudil increases GAP43 immunopositivity in the peri-infarct cortex following PT (immunohistochemistry staining).
Representative micrographs of GAP43 staining and quantification of the GAP43-positive area. Compared with the PT group, GAP43 immunopositivity was significantly higher in the PT + EE + fasudil group at 22 days after surgery. Scale bars: 100 μm, original magnification 10× (upper); 50 μm, original magnification 20× (lower). Data are expressed as the mean ± SEM (n = 3). ***P < 0.001 (one-way ANOVA followed by Tukey's multiple comparisons). EE: enriched environment; PT: photothrombotic stroke. Sham group: mice received saline; PT group: mice received photochemical embolization and saline; PT + EE group (PE): mice received photochemical embolization, EE intervention, and saline; PT + fasudil group (PF): mice received photochemical embolization and fasudil treatment at 10 mg/kg per day for 3 weeks; and PT + EE + fasudil group (PEF): mice received photochemical embolization, EE intervention, and fasudil treatment at 10 mg/kg per day for 3 weeks.

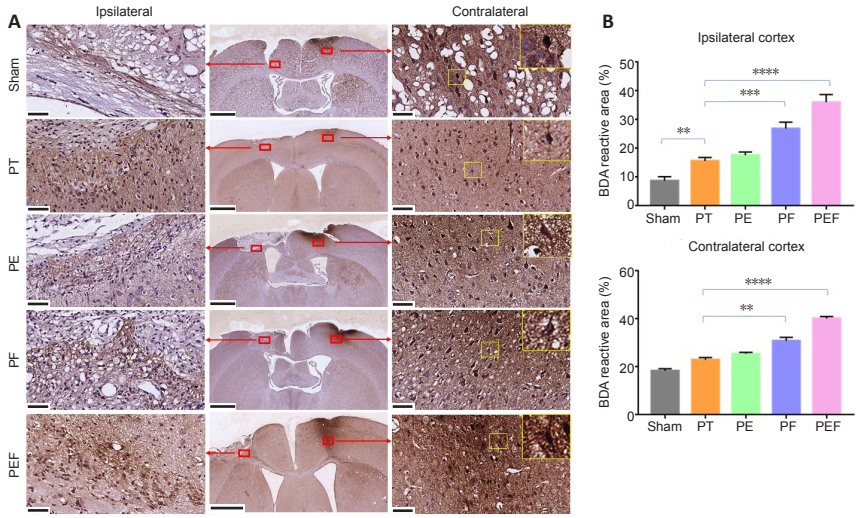

Figure 5 | EE combined with fasudil increases the BDA-labeled neurons and axons in the bilateral cortex following PT (immunohistochemical staining).
(A) Representative micrographs of BDA-labeled neurons and axons in the bilateral cortex. (B) Quantification of the BDA-reactive area in the bilateral cortex. BDA-labeled neurons and axon fibers were observed in the contralesional cortex, whereas only BDA-labeled axon fibers were observed in the ipsilesional cortex. The PT + fasudil and PT + EE + fasudil groups had greater areas of labeled neurons and sprouting axons compared with the PT group in both the contralesional and ipsilesional cortices. Scale bars: 50 μm, and 20 μm in the enlarged part. Data are expressed as the mean ± SEM (n = 3). **P < 0.01, ***P < 0.001, ****P < 0.0001 (one-way analysis of variance followed by Tukey's multiple comparisons). BDA: Biotinylated dextran amines; EE: enriched environment; PT: photothrombotic stroke. Sham group: mice received saline; PT group: mice received photochemical embolization and saline; PT + EE group (PE): mice received photochemical embolization, EE intervention, and saline; PT + fasudil group (PF): mice received photochemical embolization and fasudil treatment at 10 mg/kg per day for 3 weeks; and PT + EE + fasudil group (PEF): mice received photochemical embolization, EE intervention, and fasudil treatment at 10 mg/kg per day for 3 weeks.

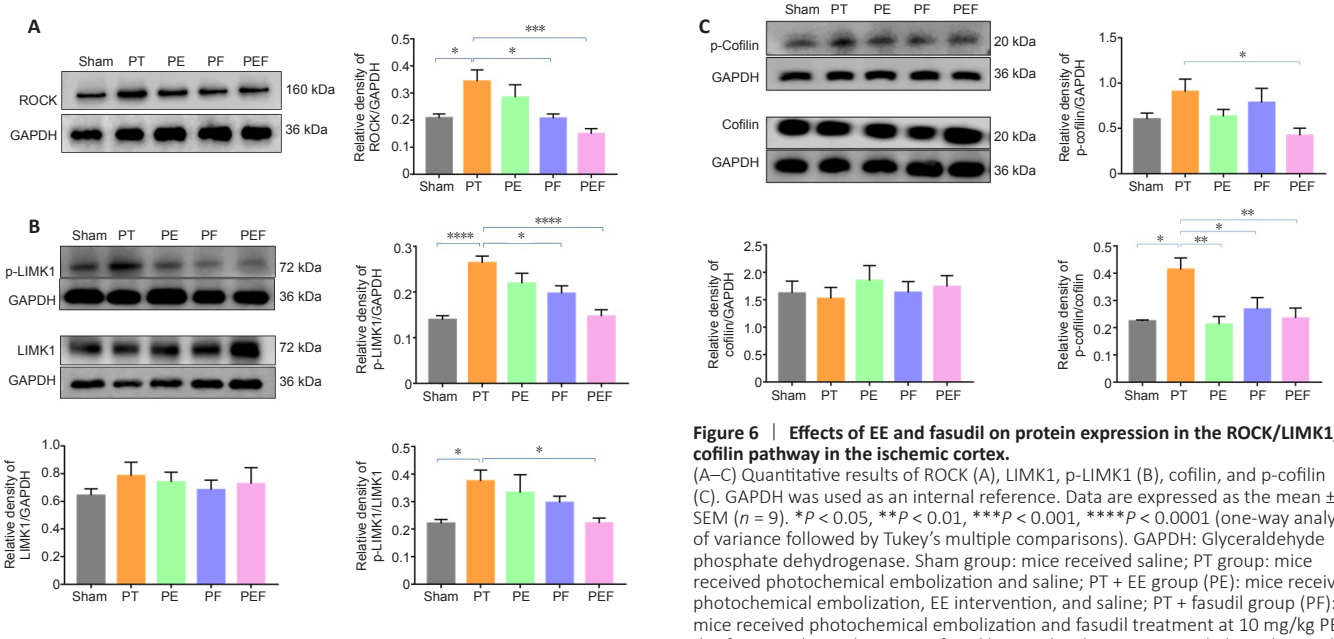

Figure 6 | Effects of EE and fasudil on protein expression in the ROCK/LIMK1/cofilin pathway in the ischemic cortex.
(A–C) Quantitative results of ROCK (A), LIMK1, p-LIMK1 (B), cofilin, and p-cofilin (C). GAPDH was used as an internal reference. Data are expressed as the mean ± SEM (n = 9). *P < 0.05, **P < 0.01, ***P < 0.001, ****P < 0.0001 (one-way analysis of variance followed by Tukey's multiple comparisons). GAPDH: Glyceraldehyde phosphate dehydrogenase. Sham group: mice received saline; PT group: mice received photochemical embolization and saline; PT + EE group (PE): mice received photochemical embolization, EE intervention, and saline; PT + fasudil group (PF): mice received photochemical embolization and fasudil treatment at 10 mg/kg PER day for 3 weeks; and PT + EE + fasudil group (PEF): mice received photochemical embolization, EE intervention, and fasudil treatment at 10 mg/kg PER day for 3 weeks.

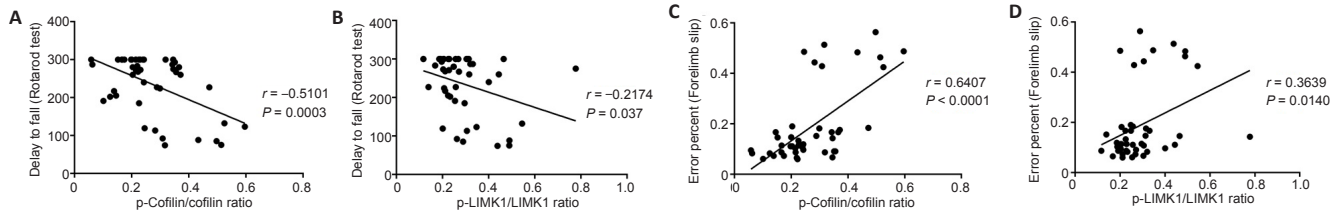

Figure 7 | **Correlation of motor function with the relative expression levels of p-cofilin/cofilin and p-LIMK1/LIMK1.**
(A, B) Correlation of rotarod results with the relative levels of p-cofilin/cofilin and p-LIMK1/LIMK1 (r = −0.5101, P = 0.0003; r = −0.3174, P = 0.037). (C, D) Correlation of forelimb slip rate with the relative levels of p-cofilin/cofilin and p-LIMK1/LIMK1 (r = 0.6407, P < 0.0001; r = 0.3639, P = 0.0140). Correlations were analyzed using Pearson's correlation coefficient method. r: Pearson's correlation coefficient

Discussion

In the present study, we performed an EE intervention in the subacute phase of cerebral ischemia (from day 7 after stroke) and attempted to fill the gap in rehabilitation during the acute phase using intraperitoneal injections of fasudil (from day 2 after stroke). The results demonstrated that early treatment with fasudil combined with delayed EE in post-stroke mice promoted motor function recovery and stimulated axonal sprouting and connections via the ROCK/LIMK1/cofilin signaling pathway. Our results revealed that this combined intervention is more effective than monotherapy in ameliorating the long-term neurological outcomes after stroke. They also provide a new therapeutic strategy for a full cycle of rehabilitation for neural functional recovery after stroke.

EE has been demonstrated as an important neurorehabilitation intervention method in basic experiments. Compared with a standard environment, EE provides more physical and social stimuli for animals (Kim et al., 2000), thereby producing a benign environment for axonal regeneration. However, the timing of EE intervention after cerebral ischemia is very important. Preliminary experimental results revealed that, although the vital signs of cerebral ischemia model rats stabilize during the acute phase of cerebral ischemia (within 24 hours after the model is created), the prognosis of motor function is worse if EE intervention is started at this time. This finding is consistent with data from many recent studies that suggest that premature acceptance of EE and other rehabilitation treatments can increase the inflammatory response in the acute phase of cerebral ischemia; this is not conducive to the growth of nerve fibers or the formation of functional connections (Wahl et al., 2019). The present study aimed to identify a suitable drug to fill the gap between injury and EE treatment in the early phase of stroke. Fasudil is the only ROCK inhibitor in clinical use that dilates cerebral blood vessels, protects nerve cells, and promotes axonal regeneration (Lingor et al., 2007). Fasudil is currently being assessed in clinical trials for the treatment of vasospasm (Zhao et al., 2011) and diseases such as amyotrophic lateral sclerosis (Takata et al., 2013), autoimmune encephalomyelitis (Yan et al., 2019), and spinal cord injury (Fu et al., 2016). Pretreatment with fasudil prior to stroke (Rikitake et al., 2005; Yamashita et al., 2007), its administration from 5 minutes to 6 hours after stroke (Huang et al., 2008; Gibson et al., 2014), and fasudil treatment starting 3 days after stroke can all achieve functional recovery (Lemmens et al., 2013). We therefore chose fasudil combined with EE as the intervention method in mice after cerebral ischemia in the present experiment. During the 3-week administration period, no adverse effects such as nausea, vomiting, respiratory depression, or coma were observed.

An ideal cerebral ischemic mouse model is important for the study of stroke. Here, a mouse model of PT was used to explore the therapeutic potential and mechanisms of fasudil combined with EE after stroke. The PT model was established with an intact skull by irradiating the corresponding cortical area with a cold light after the injection of rose bengal, which causes oxidative stress in the exposed regions, endothelial vascular damage, platelet activation, capillary closure, and secondary ischemia (Carmichael, 2005). The illumination area can be modified according to the experimental aim to cause different limb movement disorders (Kim et al., 2000). Within a few hours after the light exposure, T cells and microglia/macrophages are activated, infiltrate the injury site, and secrete large amounts of cytokines (Jander et al., 2000). Unlike the traditional middle cerebral artery occlusion model, the PT model lacks an ischemic penumbral zone and collateral circulation. The infarct area is therefore relatively fixed, and the necrosis of brain tissue is more thorough (Labat-gest and Tomasi, 2013). Moreover, the infarct area and severity can be controlled by changing the location of the fluorescence irradiation, or by adjusting the aperture or duration of irradiation (Carmichael, 2005). The drawback is that some small ischemic foci occur after small blood vessel damage, and light-associated damage in endothelial cells can destroy the integrity of blood vessels, leading to angioedema (Watson et al., 1985). However, the PT model has a relatively small cortical lesion area and a long survival time, and is therefore appropriate for the study of axonal regeneration.

The primary finding of the present study was the efficacies of both the individual interventions and the combination of EE and fasudil in ameliorating post-stroke motor impairment. The results indicated that the combination of EE and fasudil resulted in significant improvements in the rotarod test at 14 and 21 days post-stroke, whereas mice administered EE or fasudil alone still had a gap in their abilities compared with the sham mice. Similar performances were observed in the cylinder test and the rung walking test. Notably, mice in the PT + EE or PT + fasudil groups recovered relatively fast on the rotarod and rung walking tests (within 2 weeks), while in the cylinder test, the single intervention groups had no obvious effects, and the effects of the combined intervention only began to appear at week 2. This may be because the cylinder test is a sensorimotor cortex-dependent behavioral assay, and joint intervention may therefore lead to better motor coordination and fine motor ability; however, additional investigations are required.

The main factors affecting axonal regeneration in the CNS include reduced neuronal intrinsic growth ability and the influence of external factors of axonal growth. For the latter, the lack of nerve support in the adult CNS and the unfavorable environment surrounding the lesion play an important role. A pioneering study by David and Aguayo (David and Aguayo, 1981) revealed that when autologous sciatic nerve fragments of adult rats are transplanted into the injured spinal cord, the cut axons appear to re-grow. These results indicate that mature neurons retain a certain regenerative capacity, and that the surrounding unfavorable CNS environment may promote axonal regeneration after induction and regulation.

GAP43 is a specific membrane protein in the nervous system that is regulated by specific F-actin. It plays an important role in the growth and differentiation of neurons through

extracellular signals. It is highly expressed at the end of the axonal growth cone and has a guiding effect on axonal growth, thus representing a reliable marker of axonal growth (Shen et al., 2002). GAP43 expression also reflects the sprouting of axons (Skene, 1989). Under normal circumstances, GAP43 expression in mature axons of the CNS is relatively low; however, when an axon is damaged and then regenerates, GAP43 expression is re-induced (Schreyer and Skene, 1991). Therefore, GAP43 is considered a dependable indicator of axonal regeneration. Axonal regeneration mainly consists of two elements: growth and remodeling. A sufficient number of axons is a prerequisite to their ordering. In the present study, immunohistochemical staining of GAP43 revealed that fasudil effectively promoted the axonal protrusion buds, while the orderly shaping of axons was mainly accomplished by EE.

Axons usually regenerate in the following two ways. The first is that the broken end of a damaged axon continues to grow and extends toward the injured area. Here, axonal regeneration is slow, and is easily blocked by glial scars in the injured area. The second way is to generate new branches from surrounding normal neurons or axons to control the damaged area. Because axonal structure remains relatively intact close to the injury site, regenerated axons can quickly extend to the injury area to compensate for reduced innervation. It is currently believed that the nerve repair process is dominated by the second method of regeneration (Fawcett and Verhaagen, 2018). To explore the potential mechanisms underlying the appearance of motor recovery, we injected the neuronal tracer BDA into the motor area of the cerebral cortex opposite the infarct area, to observe the growth of neuronal axons in the peripheral area of the infarct. In the PT + EE + fasudil group, more labeled neuronal axons appeared in the peripheral area of the infarct compared with the PT + EE group, and these were arranged in a more orderly fashion compared with the PT + fasudil group. These findings suggest that axons from contralateral neurons grow toward the affected side through the corpus callosum to compensate for the lack of function.

The Rho/ROCK signaling pathway is an important signal transduction system in the CNS, and is widely involved in processes such as cell growth, differentiation, and migration, as well as development (Stankiewicz and Linseman, 2014). Numerous signaling molecules transmit external signals through axonal surface receptors and jointly control the Rho/ROCK signaling pathway through complex signaling networks. This results in the reorganization of the cellular actin skeleton and the collapse and retraction of the growth cone, thus affecting biological processes such as axonal projection, guidance, and extension, and nerve regeneration (Abeysinghe et al., 2016). The present study demonstrated that EE combined with fasudil treatment regulated the ROCK/LIMK1 pathway, reduced the p-cofilin/cofilin ratio, and further promoted actin filament extension and dendritic spine formation. Compared with fasudil treatment only, the effects of EE on ROCK and LIMK1 were less obvious. However, EE led to significantly reduced cofilin phosphorylation levels, suggesting that the action site of EE is downstream of this pathway. We speculate that there may have been an interaction between fasudil and EE; that is, fasudil stimulated the structural remodeling of axons, while EE promoted the functional remodeling of sprouting axons. Furthermore, the correlations between motor function improvement and the relative p-cofilin/cofilin and p-LIMK1/LIMK1 ratios in the ipsilesional cortex were analyzed. Motor performance was negatively correlated with the p-cofilin/cofilin and p-LIMK1/LIMK1 ratios, and the correlation with p-cofilin/cofilin was stronger than that of p-LIMK1/LIMK1.

In both the behavioral and molecular biology experiments, we observed the amplification effects of joint intervention. However, these effects did not always exist. For example, in Nissl staining and in the western blot detection of cofilin phosphorylation, monotherapy achieved the desired effect. The underlying reason may be related to the relatively mild damage that occurs in the PT model, as well as the detected parameters, which were all around the infarct area. This latter point is also the major limitation of the present study. We only observed changes in the cortex, and did not track the complete corticospinal tract. In follow-up experiments, we will perform long-term anterograde tracing to the cervical spinal cord to observe the regeneration of axons in this region in each group. In addition, there were some artificial deviations in this experiment—mainly in the immunohistochemical experiments—and we only used visual observation to determine whether EE aided in the orderly arrangement of the regenerated axons. In the future, we need to find ways to quantify the mechanisms underlying the effects of EE.

The current study took axonal regeneration and functional reconstruction as an entry point after cerebral ischemic injury, and examined the role of EE supplemented with a ROCK inhibitor in axonal regeneration. At the molecular level, EE combined with fasudil mediated axonal growth by inhibiting the Rho/ROCK pathway. At the structural level, neurotracing and immunohistochemical techniques were used to assess the effects of axonal structure reconstruction and to locate the initially compensated functional areas of the cerebral cortex. At the functional level, the motor function of mouse limbs was assessed and the relationship between the degree of recovery and axonal regeneration was examined, thereby clarifying the mechanisms by which EE might integrate the new axons induced by ROCK inhibitors. Our results provide a translational reference for defining comprehensive treatment plans of post-stroke medicine combined with rehabilitation training, as well as a new basis for improving the functional compensation theory of stroke rehabilitation.

Author contributions: *Experiment implementation: YTZ, GJX, YW; data collection: YTZ, YW; data analysis: QZ, KWY; manuscript writing: YTZ; manuscript revision: HYX, SYL; guidance: QZ, YW. All authors approved the final version of the manuscript.*
Conflicts of interest: *The authors declared that they have no conflicts of interest to this work.*
Financial support: *This study was supported by the National Natural Science Foundation of China, Nos. 81672242 (to YW), 81972141 (to YW); Shanghai Sailing Program, No. 20YF1403500 (to QZ); and Shanghai Municipal Key Clinical Specialty of China, No. shslczdzk02702 (to YW). The funding sources had no role in study conception and design, data analysis or interpretation, paper writing or deciding to submit this paper for publication.*
Institutional review board statement: *This study was approved by the Institutional Animal Care and Use Committee of Fudan University (Shanghai, China; approval No. 20160858A232) on February 24, 2016.*

Data sharing statement: *Datasets analyzed during the current study are available from the corresponding author on reasonable request.*
Plagiarism check: *Checked twice by iThenticate.*
Peer review: *Externally peer reviewed.*

Open peer reviewer: *Sumana Chakravarty, Indian Institute of Chemical Technology, India.*
Additional files:
Additional file 1: *Open peer review report 1.*
Additional file 2: *Original data of the experiment*

References

Abeysinghe HC, Phillips EL, Chin-Cheng H, Beart PM, Roulston CL (2016) Modulating astrocyte transition after stroke to promote brain rescue and functional recovery: emerging targets include Rho kinase. Int J Mol Sci 17:288.

AVERT Trial Collaboration group (2015) Efficacy and safety of very early mobilisation within 24 h of stroke onset (AVERT): a randomised controlled trial. Lancet 386:46-55.

Bernstein BW, Bamburg JR (2010) ADF/cofilin: a functional node in cell biology. Trends Cell Biol 20:187-195.

Blackmore MG, Wang Z, Lerch JK, Motti D, Zhang YP, Shields CB, Lee JK, Goldberg JL, Lemmon VP, Bixby JL (2012) Krüppel-like factor 7 engineered for transcriptional activation promotes axon regeneration in the adult corticospinal tract. Proc Natl Acad Sci U S A 109:7517-7522.

Brabeck C, Mittelbronn M, Bekure K, Meyermann R, Schluesener HJ, Schwab JM (2003) Effect of focal cerebral infarctions on lesional RhoA and RhoB expression. Arch Neurol 60:1245-1249.

Cai DX, Zeng Q, He LL, Huang GZ (2020) Application and mechanism of virtual reality technology in post-stroke rehabilitation of the hemiplegic upper limb. Zhongguo Zuzhi Gongcheng Yanjiu 24:5228-5235.

Campbell BCV, De Silva DA, Macleod MR, Coutts SB, Schwamm LH, Davis SM, Donnan GA (2019) Ischaemic stroke. Nat Rev Dis Primers 5:70.

Carmichael ST (2005) Rodent models of focal stroke: size, mechanism, and purpose. NeuroRx 2:396-409.

David S, Aguayo AJ (1981) Axonal elongation into peripheral nervous system "bridges" after central nervous system injury in adult rats. Science 214:931-933.

de Oliveira JL, Ávila M, Martins TC, Alvarez-Silva M, Winkelmann-Duarte EC, Salgado ASI, Cidral-Filho FJ, Reed WR, Martins DF (2020) Medium- and long-term functional behavior evaluations in an experimental focal ischemic stroke mouse model. Cogn Neurodyn 14:473-481.

Fawcett JW, Verhaagen J (2018) Intrinsic determinants of axon regeneration. Dev Neurobiol 78:890-897.

Fu PC, Tang RH, Wan Y, Xie MJ, Wang W, Luo X, Yu ZY (2016) ROCK inhibition with fasudil promotes early functional recovery of spinal cord injury in rats by enhancing microglia phagocytosis. J Huazhong Univ Sci Technolog Med Sci 36:31-36.

Gibson CL, Srivastava K, Sprigg N, Bath PM, Bayraktutan U (2014) Inhibition of Rho-kinase protects cerebral barrier from ischaemia-evoked injury through modulations of endothelial cell oxidative stress and tight junctions. J Neurochem 129:816-826.

Huang L, He Z, Guo L, Wang H (2008) Improvement of cognitive deficit and neuronal damage in rats with chronic cerebral ischemia via relative long-term inhibition of rho-kinase. Cell Mol Neurobiol 28:757-768.

Kim GW, Sugawara T, Chan PH (2000) Involvement of oxidative stress and caspase-3 in cortical infarction after photothrombotic ischemia in mice. J Cereb Blood Flow Metab 20:1690-1701.

Lemmens R, Jaspers T, Robberecht W, Thijs VN (2013) Modifying expression of EphA4 and its downstream targets improves functional recovery after stroke. Hum Mol Genet 22:2214-2220.

Lingor P, Teusch N, Schwarz K, Mueller R, Mack H, Bähr M, Mueller BK (2007) Inhibition of Rho kinase (ROCK) increases neurite outgrowth on chondroitin sulphate proteoglycan in vitro and axonal regeneration in the adult optic nerve in vivo. J Neurochem 103:181-189.

Liu YH, Zhao Y, Huang FZ, Chen YH, Wang HX, Bonney E, Liu BQ (2016) Combination of early constraint-induced movement therapy and fasudil enhances motor recovery after ischemic stroke in rats. Int J Neurosci 126:168-173.

Liu Z, Li Y, Qian J, Cui Y, Chopp M (2014) Plasminogen deficiency causes reduced corticospinal axonal plasticity and functional recovery after stroke in mice. PLoS One 9:e94505.

Morin P, Wickman G, Munro J, Inman GJ, Olson MF (2011) Differing contributions of LIMK and ROCK to TGFβ-induced transcription, motility and invasion. Eur J Cell Biol 90:13-25.

Mu J, Bakreen A, Juntunen M, Korhonen P, Oinonen E, Cui L, Myllyniemi M, Zhao S, Miettinen S, Jolkkonen J (2019) Combined adipose tissue-derived mesenchymal stem cell therapy and rehabilitation in experimental stroke. Front Neurol 10:235.

Paxinos G, Franklin KB (2013) The mouse brain in stereotaxic coordinates. San Diego: Elsevier.

Rikitake Y, Kim HH, Huang Z, Seto M, Yano K, Asano T, Moskowitz MA, Liao JK (2005) Inhibition of Rho kinase (ROCK) leads to increased cerebral blood flow and stroke protection. Stroke 36:2251-2257.

Rosbergen IC, Grimley RS, Hayward KS, Brauer SG (2019) The impact of environmental enrichment in an acute stroke unit on how and when patients undertake activities. Clin Rehabil 33:784-795.

Schmandke A, Schmandke A, Strittmatter SM (2007) ROCK and Rho: biochemistry and neuronal functions of Rho-associated protein kinases. Neuroscientist 13:454-469.

Schreyer DJ, Skene JH (1991) Fate of GAP-43 in ascending spinal axons of DRG neurons after peripheral nerve injury: delayed accumulation and correlation with regenerative potential. J Neurosci 11:3738-3751.

Shen Y, Mani S, Donovan SL, Schwob JE, Meiri KF (2002) Growth-associated protein-43 is required for commissural axon guidance in the developing vertebrate nervous system. J Neurosci 22:239-247.

Skene JH (1989) Axonal growth-associated proteins. Annu Rev Neurosci 12:127-156.

Stankiewicz TR, Linseman DA (2014) Rho family GTPases: key players in neuronal development, neuronal survival, and neurodegeneration. Front Cell Neurosci 8:314.

Takata M, Tanaka H, Kimura M, Nagahara Y, Tanaka K, Kawasaki K, Seto M, Tsuruma K, Shimazawa M, Hara H (2013) Fasudil, a rho kinase inhibitor, limits motor neuron loss in experimental models of amyotrophic lateral sclerosis. Br J Pharmacol 170:341-351.

Wahl AS, Erlebach E, Brattoli B, Büchler U, Kaiser J, Ineichen BV, Mosberger AC, Schneeberger S, Imobersteg S, Wieckhorst M, Stirn M, Schroeter A, Ommer B, Schwab ME (2019) Early reduced behavioral activity induced by large strokes affects the efficiency of enriched environment in rats. J Cereb Blood Flow Metab 39:2022-2034.

Wang X, Meng ZX, Chen YZ, Li YP, Zhou HY, Yang M, Zhao TT, Gong YL, Wu Y, Liu T (2020) Enriched environment enhances histone acetylation of NMDA receptor in the hippocampus and improves cognitive dysfunction in aged mice. Neural Regen Res 15:2327-2334.

Wang Z, Reynolds A, Kirry A, Nienhaus C, Blackmore MG (2015) Overexpression of Sox11 promotes corticospinal tract regeneration after spinal injury while interfering with functional recovery. J Neurosci 35:3139-3145.

Watson BD, Dietrich WD, Busto R, Wachtel MS, Ginsberg MD (1985) Induction of reproducible brain infarction by photochemically initiated thrombosis. Ann Neurol 17:497-504.

Winstein CJ, Stein J, Arena R, Bates B, Cherney LR, Cramer SC, Deruyter F, Eng JJ, Fisher B, Harvey RL, Lang CE, MacKay-Lyons M, Ottenbacher KJ, Pugh S, Reeves MJ, Richards LG, Stiers W, Zorowitz RD; American Heart Association Stroke Council; Council on Cardiovascular and Stroke Nursing, et al. (2016) Guidelines for Adult Stroke Rehabilitation and Recovery: a guideline for healthcare professionals from the American Heart Association/American Stroke Association. Stroke 47:e98-e169.

Xie H, Wu Y, Jia J, Liu G, Zhang F, Zhang Q, Yu K, Hu Y, Bai Y, Hu R (2013) Enriched environment preconditioning induced brain ischemic tolerance without reducing infarct volume and edema: the possible role of enrichment-related physical activity increase. Brain Res 1508:63-72.

Yamashita K, Kotani Y, Nakajima Y, Shimazawa M, Yoshimura S, Nakashima S, Iwama T, Hara H (2007) Fasudil, a Rho kinase (ROCK) inhibitor, protects against ischemic neuronal damage in vitro and in vivo by acting directly on neurons. Brain Res 1154:215-224.

Yan Y, Yu J, Gao Y, Kumar G, Guo M, Zhao Y, Fang Q, Zhang H, Yu J, Jiang Y, Zhang HT, Ma CG (2019) Therapeutic potentials of the Rho kinase inhibitor Fasudil in experimental autoimmune encephalomyelitis and the related mechanisms. Metab Brain Dis 34:377-384.

Yano K, Kawasaki K, Hattori T, Tawara S, Toshima Y, Ikegaki I, Sasaki Y, Satoh S, Asano T, Seto M (2008) Demonstration of elevation and localization of Rho-kinase activity in the brain of a rat model of cerebral infarction. Eur J Pharmacol 594:77-83.

Zhang Q, Wu JF, Shi QL, Li MY, Wang CJ, Wang X, Wang WY, Wu Y (2019) The neuronal activation of deep cerebellar nuclei is essential for environmental enrichment-induced post-stroke motor recovery. Aging Dis 10:530-543.

Zhao J, Zhou D, Guo J, Ren Z, Zhou L, Wang S, Zhang Y, Xu B, Zhao K, Wang R, Mao Y, Xu B, Zhang X (2011) Efficacy and safety of fasudil in patients with subarachnoid hemorrhage: final results of a randomized trial of fasudil versus nimodipine. Neurol Med Chir (Tokyo) 51:679-683.

P-Reviewer: Chakravarty S; C-Editor: Zhao M; S-Editors: Yu J, Li CH; L-Editors: Gardner B, Yu J, Song LP; T-Editor: Jia Y